Reliability Engineering and System Safety 180 (2018) 345–351

Contents lists available at ScienceDirect

Reliability Engineering and System Safety

journal homepage: www.elsevier.com/locate/ress

Dynamic reliability modeling for system analysis under complex load

Xiaoqiang Zhang[a,b], Huiying Gao[c], Hong-Zhong Huang[a,b,*], Yan-Feng Li[a,b], Jinhua Mi[a,b]

[a] School of Mechanical and Electrical Engineering, University of Electronic Science and Technology of China, Chengdu 611731, China
[b] Center for System Reliability and Safety, University of Electronic Science and Technology of China, Chengdu 611731, China
[c] School of Automobile & Transportation, Xihua University, Chengdu 610039, China

ARTICLE INFO

Keywords:
Dynamic reliability modeling
Shock load
Nonhomogeneous poisson process
Gauss–Legendre quadrature formula

ABSTRACT

The traditional stress-strength interference (SSI) model regards the strength and the stress as two continuous random variables, but in practical engineering, the strength may be a stochastic degradation process. Besides continuous working load, a mechanical system often suffers from shock loads as well. How to calculate the dynamical reliability under complex load is a challenge that needs to be resolved. This paper proposes a generalized dynamic reliability model for the calculation of system reliability under complex load. The proposed model is available for system reliability problems under deterministic strength degradation or stochastic strength degradation processes. Six sigma and Gauss-Legendre quadrature formula are adopted to calculate the system reliability. A case study under three different conditions is presented to illustrate the application of the proposed model. The accuracy of the proposed method is compared with MCS.

1. Introduction

In mechanical products, the working condition of a component (or system) is interacted by the generalized strength and the stress. Herein, the generalized stress has a wide scope such as displacement, temperature, force, pressure, and vibration, which can induce failures, and the strength implies the ability to resist the failures. When the stress is less than the strength, the component (or system) works properly; otherwise, failure occurs [1]. The stress-strength interference (SSI) method is one of the commonly used methods for structural reliability analysis. The existing methods such as the first-order reliability method (FORM), the second-order reliability method (SORM) and simulation techniques (which are applicable to a broader class of problems with less restrictive assumptions) are now available, but the SSI method is still a popular method for its simple form and computational simplicity. The traditional SSI model regards the strength and the stress as two continuous random variables, the failure will occur when the probability density function (PDF) of strength and stress overlap.

The SSI is the basis of reliability modeling based on physics of failure (PoF). Many efforts have been made to improve the traditional SSI model and extend the scope of its application. So far, the methods for reliability modeling are divided into two types: static modeling and dynamic modeling. The static modeling methods contain Reliability Block Diagram (RBD), Fault Tree (FT) [2], and Binary Decision Diagram (BDD) [3]. Dynamic reliability modeling gained extensive attention and a large amount of research works have been done during the past decades. For dynamic reliability analysis, the available reliability analysis methods can be roughly classified into three categories: up-crossing rate methods/first-passage methods, analytical methods do not based on up-crossing rate, and the sampling-based methods. The well-known first-passage formula has established the foundation for the concept of first-passage failure in dynamic reliability theory [4]. However, the first-passage formula is hard to use in real applications because of its complicated integral operation. Subsequently, a new method was proposed to calculate the first-passage probability for structure based on continuous Markov process [5] and the analytical solution for the first-passage time was derived [6]. However, the above two methods are only applicable to some specific cases of the limit-state functions. Coleman [7] proposed Poisson-based approximation for first-passage frequency calculations. Poisson-based approximation has built a bridge between the up-crossing rates and the dynamical reliability of the structure; however, its accuracy is based on a precondition that the crossings of the structural responses from the safety state to the failure state belong to rare events and furthermore they should be independent from each other. Crandall et al. [8] introduced the numerical simulation method for solving the first-passage problem. Spanos and Kougioumtzoglou [9] studied the first-passage method for a class of lightly damped nonlinear oscillators under random excitations. Rackwitz [10] and Melchers and Beck [11] applied the outcrossing rate method to address dynamic uncertain loads in time-variant reliability problems. Hu and Du [12] developed a more accurate method for time-dependent reliability analysis with joint up-crossing rates to consider the dependence of up-crossings. Jiang et al. [13] proposed

* Corresponding author at: School of Mechanical and Electrical Engineering, University of Electronic Science and Technology of China, Chengdu 611731, China.
E-mail address: hzhuang@uestc.edu.cn (H.-Z. Huang).

https://doi.org/10.1016/j.ress.2018.07.025
Received 28 March 2017; Received in revised form 20 June 2018; Accepted 25 July 2018
Available online 02 August 2018

ACRONYMS

SSI	stress-strength interference
PDF	probability density function
FORM	first-order reliability method
SORM	second-order reliability method
RBD	reliability block diagram
FT	fault tree
BDD	binary decision diagram
PoF	physics of failure
MCS	Monte Carlo simulation

NOTATIONS

$L_o(\mathbf{C}, t)$	continuous working load, a stochastic process
$S(\mathbf{\Phi}, t)$	strength degradation model, a function of t and $\mathbf{\Phi}$
$\mathbf{C} = (C_1, C_2, \ldots)$	a variable vector, related to working load
$\Phi = (\varphi_1, \varphi_2, \ldots)$	a variable vector, related to strength
t	time instant or service duration
$f_{\mathbf{C}}(\mathbf{c})$	joint probability density function of random variables $C_1, C_2, \ldots$
$f_{\mathbf{\Phi}}(\boldsymbol{\varphi})$	joint probability density function of random variables $\varphi_1, \varphi_2, \ldots$
$\lambda(t)$	intensity function of Poisson process
L_s	the shock load, a random variable
μ_{L_s}	mean value of shock load
σ_{L_s}	standard deviation of shock load
$L_{o+s}(\mathbf{C}, t)$	complex load, equals the sum of working load and the shock load
$R(t)$	reliability in a service duration
Δt	time increment
$K(t)$	shock load occurs at time instant t
$\overline{K}(t)$	shock load does not occur at time instant t
$f_{L_{o+s}}(\cdot)$	PDF of complex load
x_k	Gauss-Legendre integration points
A_k	Gauss-Legendre integration coefficients

a time-dependent system reliability analysis method, which transformed the evaluation of the system outcrossing rates into the calculation of a time-invariant system reliability. Andrieu-Renaud et al. [14] proposed the PHI2 method to calculate outcrossing rates, and this method is simple and easy to understand. However, the computational efficiency may decrease for some complex or nonstationary problems. Zhang et al. [15] proposed a response surface based time-dependent reliability analysis method for structures under stochastic loads. Li and Mourelatos [16] used a niching genetic algorithm to calculate time-variant reliability in power problems. Singh et al. [17] proposed an importance sampling method for time-variant reliability analysis. Jiang et al. [18] proposed a novel time-variant reliability analysis method based on stochastic process discretization, which is effective for complex structures. Wang et al. [19] proposed a simulation based method to estimate two types of time-varying failure rate of dynamic systems. Peng et al. [20] used inverse Gaussian process models and Bayesian degradation for time-varying degradation rates. Mourelatos et al. [21] proposed a reliability analysis method for time-dependent problems using the total probability theorem and the concept of composite limit state. Hu and Du [22] proposed a sampling approach to obtain the extreme value distribution of a stochastic process, which can calculate the dynamic reliability efficiently. Mi et al. [23] proposed a belief universal generating function analysis method of multi-state systems under epistemic uncertainty and common cause failures. Wang and Wang [24] proposed a time-dependent reliability-based design optimization method based on a nested extreme response surface technique. Recently, Zayed et al. [25] carried out the time-variant reliability assessment for ship structures using the fast integration techniques. Mi et al. [26] proposed a reliability analysis method for complex multi-state system with common cause failure. Liu et al. [27] introduced detailed comparisons of the two non-probabilistic structural reliability analysis methods on aspects such as modeling ideas, model structures, precision, etc. Wang and Wang [28] proposed a confidence-based meta-modeling approach for efficient sensitivity-free dynamic reliability analysis. Guo et al. [29] proposed a Bayesian degradation assessment of CNC machine tools considering unit non-homogeneity. Park [30] derived the time-dependent reliabilities of the wireless networks with dependent failures. Mi et al. [31] proposed reliability assessment of complex electromechanical systems under epistemic uncertainty. Li et al. [32] proposed a dynamic reliability assessment method for multi-state phased mission system with non-repairable multi-state components. Yang et al. [33] proposed a Bayesian approach for sealing reliability analysis considering the non-competing relationship of multiple degradation processes.

Although many aforementioned studies have been done, the shock loads which may happen in the service of mechanical products are not considered. In this paper, a generalized dynamic reliability model is developed under complex load profile. The model is not only applicable to homogeneous Poisson loading processes with normally distributed load amplitudes, but also can deal with nonhomogeneous Poisson loads. For a system under stochastic strength degradation and stochastic load, it is very difficult to calculate system reliability by the direct integral methods. In this paper, six sigma and Gauss-Legendre quadrature formula are used to calculate the system reliability.

The rest of this article is organized as follows. Section 2 lists some assumptions on which the established dynamic reliability model is based. A generalized dynamic reliability model for systems under complex load is proposed in Section 3. Section 4 provides a numerical integration method for dynamic reliability calculation. A case study under different conditions is presented in Section 5. Conclusions are finally summarized in Section 6.

2. Assumptions

In this paper, the generalized dynamic reliability model is established under some assumptions as follows:

(1) The working load follows a stochastic process $L_o(\mathbf{C}, t)$ and the strength degradation can be modeled as a stochastic process $S(\mathbf{\Phi}, t)$.
(2) The working load, strength degradation and shock loads are statistically independent from each other.
(3) Denote that $\mathbf{C} = (C_1, C_2, \cdots, C_m)$ and $\Phi = (\varphi_1, \varphi_2, \ldots, \varphi_n)$. Random variables c_i/φ_i with known PDFs in random variable vector $\mathbf{C}/\mathbf{\Phi}$ are independent from each other. Then, $f_{\mathbf{C}}(\mathbf{c}) = \prod_{i=1}^{m} f_{C_i}(c_i)$, $f_{\Phi}(\varphi) = \prod_{i=1}^{n} f_{\Phi_i}(\varphi_i)$, where m and n are the numbers of random variables in $\mathbf{C}$ and $\mathbf{\Phi}$, respectively.
(4) The arrivals of shock loads in a certain time interval that follows a Poisson process with intensity $\lambda(t)$. The amplitudes of shock loads follow a normal distribution with mean μ_{L_s} and standard deviation σ_{L_s}.

3. The generalized dynamic reliability model

In practical engineering, besides continuous working loads, a mechanical product is often subjected to discrete shock loads as well. If the discrete shock loads appear at time instant t, the product bears a total load that equals to the sum of two loads, i.e., $L_{o+s}(\mathbf{C}, t) = L_o(\mathbf{C}, t) + L_s$; otherwise, the product bears continuous working loads only, $L_{o+s}(\mathbf{C}, t) = L_o(\mathbf{C}, t)$. In the other hand, for aging or wear-out reasons, the strength of a system is often treated as a degradation process. According to the different regularities of degradation, it can be divided into deterministic degradation and stochastic degradation. Dynamic reliability models under complex load and two types of degradation are discussed in the following sections, respectively.

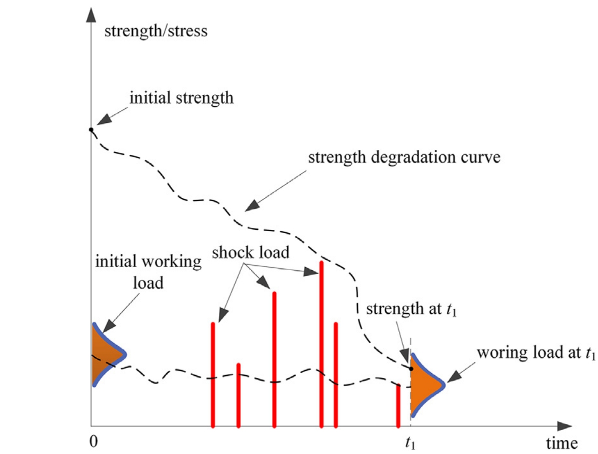

Fig. 1. The SSI model under deterministic strength degradation and complex load.

3.1. Deterministic degradation process

For a given system, the continuous working load is a stochastic process and the shock load is a random variable. When the degradation process of the strength is deterministic, the strength $S(\boldsymbol{\Phi}, t)$ is a constant (not a random variable) at any given time instant. The interaction between the complex load and the strength is illustrated in Fig. 1.

According to the SSI theory, the dynamic reliability at time instant t is defined as

$$R(t) = \Pr\{L_{o+s}(\mathbf{C}, \tau) < S(\Phi, \tau), \forall \tau \in (0, t)\} \tag{1}$$

where $L_{o+s}(\mathbf{C}, t)$ is the complex load, and equals to the sum of working load and the shock load.

Let $K(t)$ be the shock load occurs at time instant t, and $\overline{K}(t)$ be the shock load does not occur. According to assumption 3, the arrivals of shock loads in a certain time interval follow a Poisson process with intensity function $\lambda(t)$.

For $\forall \tau \in (t, t + \Delta t)$, we have

$$\Pr\{K(\tau)\} = \lambda(\tau)\Delta t + o(\Delta t) \tag{2}$$

and

$$\Pr\{\overline{K}(\tau)\} = 1 - \Pr\{K(\tau)\} = 1 - \lambda(\tau)\Delta t - o(\Delta t) \tag{3}$$

The whole probability formula yields

$$\begin{aligned} R(t + \Delta t) &= R(t) \times [\Pr\{L_{o+s}(\mathbf{C}, \tau) < S(\Phi, \tau)\} \times \Pr\{K(\tau)\}] \\ &\quad + R(t) \times \Pr\{\overline{K}(\tau)\}, \forall \tau \in (t, t + \Delta t) \\ &= R(t) \times \Pr\{L_{o+s}(\mathbf{C}, \tau) < S(\Phi, \tau)\} \\ &\quad \times [\lambda(\tau)\Delta t + o(\Delta t)] + R(t) \times [1 - \lambda(\tau)\Delta t - o(\Delta t)], \forall \tau \\ &\in (t, t + \Delta t) \end{aligned} \tag{4}$$

Eq. (4) can be rewritten as

$$\begin{aligned} \frac{R(t+\Delta t) - R(t)}{\Delta t} &= R(t) \times \Pr\{L_{o+s}(\mathbf{C}, \tau) < S(\Phi, \tau)\} \times \left[\lambda(\tau) + \frac{o(\Delta t)}{\Delta t}\right] \\ &\quad - R(t) \times \left[\lambda(\tau) + \frac{o(\Delta t)}{\Delta t}\right], \forall \tau \in (t, t + \Delta t) \end{aligned} \tag{5}$$

when $\Delta t \to 0$, then $\tau \to t$, $\frac{o(\Delta t)}{\Delta t} \to 0$, and this yields

$$\frac{\mathrm{d}R(t)}{\mathrm{d}t} = R(t) \times \lambda(t) \times [\Pr\{L_{o+s}(\mathbf{C}, t) < S(\Phi, t)\} - 1] \tag{6}$$

Noting that $R(0) = 1$, solving the differential equation in Eq. (6) yields

$$\begin{aligned} R(t) &= e^{\int_0^t \lambda(\xi) \times [\Pr\{L_{o+s}(\mathbf{C}, \xi) < S(\Phi, \xi)\} - 1]\mathrm{d}\xi} \\ &= e^{\int_0^t \lambda(\xi) \times \left[\int_{-\infty}^{S(\Phi,\xi)} f_{L_{o+s}}(\mathbf{C}, \xi)\mathrm{d}\mathbf{C} - 1\right]\mathrm{d}\xi} \end{aligned} \tag{7}$$

where $f_{L_{o+s}}(\cdot)$ is the PDF of the complex load.

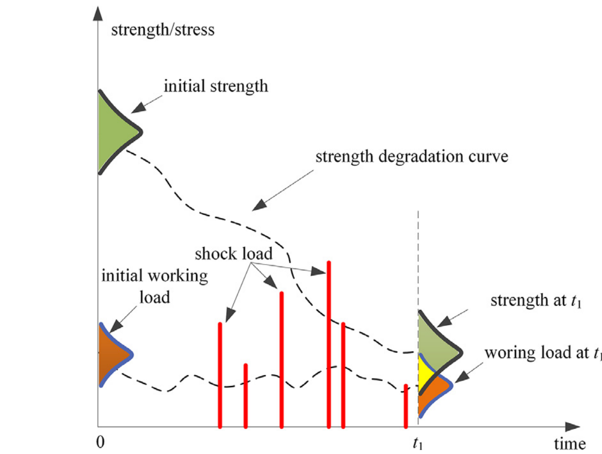

Fig. 2. The SSI model under stochastic strength degradation and complex load.

3.2. Stochastic degradation process

When the degradation of the strength is a stochastic process, the strength at any given time instant is a random variable. The whole interaction process between stochastic strength degradation, stochastic working load and random shock load is illustrated with Fig. 2.

Combining Eq. (7) with the whole probability formula yields the system reliability at time instant t as follows

$$\begin{aligned} R(t) &= \int_{\varphi} R[t | S(\Phi, t) = S(\varphi, t)] f_{\Phi}(\varphi)\mathrm{d}\varphi \\ &= \int_{\varphi} e^{\int_0^t \lambda(\xi) \times \left[\int_{-\infty}^{S(\varphi,\xi)} f_{L_{o+s}}(\mathbf{C}, \xi)\mathrm{d}\mathbf{C} - 1\right]\mathrm{d}\xi} f_{\Phi}(\varphi)\mathrm{d}\varphi \end{aligned} \tag{8}$$

Eq. (8) indicates that the system reliability under complex loads and stochastic strength degradation is no longer an exponential distribution. Formally, it is difficult to obtain an explicit expression. How to calculate $R(t)$ becomes a problem that needed to be solved. Gauss-Legendre quadrature formula will be introduced in next session to solve the problem.

4. Reliability analysis and calculation

Gauss-Legendre numerical integration possesses $2n + 1$ order accuracy [34], so we select the Gauss–Legendre quadrature formula to calculate the dynamic reliability.

For convenience, denoting $H(t, \varphi) = \lambda(t) \times [\int_{-\infty}^{S(\varphi,t)} f_{L_{o+s}}(\mathbf{C}, t)\mathrm{d}\mathbf{C} - 1]$ and $M(t, \varphi) = e^{\int_0^t H(\xi,\varphi)\mathrm{d}\xi}$, and then

$$R(t) = \int_{\varphi} M(t, \varphi) f_{\Phi}(\varphi)\mathrm{d}\varphi \tag{9}$$

and

$$M(t + \Delta t, \varphi) = e^{\int_0^{t+\Delta t} H(\xi,\varphi)\mathrm{d}\xi} = e^{\int_0^t H(\xi,\varphi)\mathrm{d}\xi + \int_t^{t+\Delta t} H(\xi,\varphi)\mathrm{d}\xi} \tag{10}$$

If the time increment Δt is small enough, we have

$$e^{\int_t^{t+\Delta t} H(\xi,\varphi)\mathrm{d}\xi} \approx e^{\frac{[H(t,\varphi) + H(t+\Delta t,\varphi)]}{2}\Delta t} \tag{11}$$

Using the Taylor series expansion, we obtain

$$\begin{aligned} & e^{\frac{[H(t,\varphi)+H(t+\Delta t,\varphi)]}{2}\Delta t} \\ &= 1 + \frac{[H(t, \varphi) + H(t + \Delta t, \varphi)]}{2}\Delta t + o(\Delta t) \end{aligned} \tag{12}$$

Substituting Eqs. (11) and (12) into Eq. (10) yields

$$\begin{aligned} M(t + \Delta t, \varphi) &\approx e^{\int_0^t H(\xi,\varphi)\mathrm{d}\xi + \frac{[H(t,\varphi)+H(t+\Delta t,\varphi)]}{2}\Delta t} \\ &= M(t, \varphi) \times e^{\frac{[H(t,\varphi)+H(t+\Delta t,\varphi)]}{2}\Delta t} \\ &\approx M(t, \varphi)\left(1 + \frac{[H(t, \varphi) + H(t + \Delta t, \varphi)]}{2}\Delta t\right) \end{aligned} \tag{13}$$

Table 1
Gauss-Legendre integration points and coefficients ($m = 11$) [35].

x_k	± 0.978229	± 0.887063	± 0.730152	± 0.519096	± 0.269543	0
A_k	0.055669	0.125580	0.186290	0.233194	0.262805	0.272925

Combining Eqs. (9) and (13) yields

$$\begin{aligned} R(t+\Delta t) &= \int_\varphi M(t+\Delta t,\varphi) f_\Phi(\varphi)\mathrm{d}\varphi \\ &\approx \int_\varphi M(t,\varphi)\times\left(1+\frac{[H(t,\varphi)+H(t+\Delta t,\varphi)]}{2}\Delta t\right) f_\Phi(\varphi)\mathrm{d}\varphi \\ &= R(t)+\frac{\Delta t}{2}\int_\varphi M(t,\varphi)[H(t,\varphi)+H(t+\Delta t,\varphi)] f_\Phi(\varphi)\mathrm{d}\varphi \end{aligned} \tag{14}$$

For a single variable, $\varphi = \varphi$, applying the Gauss-Legendre quadrature formula to the second item of Eq. (14) to yield

$$\begin{aligned} &\int_\varphi M(t,\varphi)[H(t,\varphi)+H(t+\Delta t,\varphi)] f_\Phi(\varphi)\mathrm{d}\varphi \\ &= \int_{\varphi_l}^{\varphi_u} M(t,\varphi)[H(t,\varphi)+H(t+\Delta t,\varphi)] f_\Phi(\varphi)\mathrm{d}\varphi \\ &= \frac{\varphi_u-\varphi_l}{2}\sum_{k=1}^m A_k M(t,\varphi_k)[H(t,\varphi_k)+H(t+\Delta t,\varphi_k)] f_\Phi(\varphi_k) \end{aligned} \tag{15}$$

where $\varphi_k = \frac{\varphi_u-\varphi_l}{2}x_k + \frac{\varphi_u+\varphi_l}{2}$, m is the number of nodes, x_k are the nodes of Gauss-Legendre quadrature formula, and A_k are the corresponding coefficients. The points and coefficients of Gauss-Legendre integration are listed in Table 1.

When $\boldsymbol{\varphi}$ is a vector with two random variables, $\varphi = (\varphi_1, \varphi_2)$, Quadratic Gauss-Legendre quadrature formula can be used, we have

$$\begin{aligned} &\int_\varphi M(t,\varphi)[H(t,\varphi)+H(t+\Delta t,\varphi)] f_\Phi(\varphi)\mathrm{d}\varphi \\ &= \frac{\varphi_{2U}-\varphi_{2L}}{2}\sum_{k=1}^m A_k\left\{\frac{\varphi_{1U}-\varphi_{1L}}{2}\sum_{k=1}^m A_k\{M(t,\varphi)[H(t,\varphi)+H(t+\Delta t,\varphi)] f_\Phi(\varphi)\}_{\varphi_1=\varphi_{1k}}\right\}_{\varphi_2=\varphi_{2k}} \\ &= \prod_{i=1}^2\frac{\varphi_{iU}-\varphi_{iL}}{2}\sum_{k=1}^m A_k\left\{\sum_{k=1}^m A_k\{M(t,\varphi)\cdot[H(t,\varphi)+H(t+\Delta t,\varphi)] f_\Phi(\varphi)\}_{\varphi_1=\varphi_{1k}}\right\}_{\varphi_2=\varphi_{2k}} \end{aligned} \tag{16}$$

where $\varphi_{ik} = \frac{\varphi_{iU}-\varphi_{iL}}{2}x_k + \frac{\varphi_{iU}+\varphi_{iL}}{2}$, $i = 1, 2$, m is the number of nodes, x_k are the nodes of Gauss-Legendre quadrature formula, and A_k are the corresponding coefficients.

Generalizing $\boldsymbol{\varphi}$ to n-dimensional vector $\varphi = (\varphi_1, \varphi_2, ..., \varphi_n)$ yields

$$\begin{aligned} &\int_{\boldsymbol{\varphi}} M(t,\boldsymbol{\varphi})\left[H(t,\boldsymbol{\varphi})+H(t+\Delta t,\boldsymbol{\varphi})\right] f_\Phi(\boldsymbol{\varphi})\mathrm{d}\boldsymbol{\varphi} \\ &= \prod_{i=1}^n\frac{\varphi_{iU}-\varphi_{iL}}{2}\underbrace{\sum_{k=1}^m A_k\cdots\left\{\sum_{k=1}^m A_k\right.}_{n}\cdot\left.\left\{M(t,\boldsymbol{\varphi})\left[H(t,\boldsymbol{\varphi})+H(t+\Delta t,\boldsymbol{\varphi})\right] f_\Phi(\boldsymbol{\varphi})\right\}_{\varphi_1=\varphi_{1k}}\right\}_{\ddots\,\varphi_n=\varphi_{nk}} \end{aligned} \tag{17}$$

Combining Eqs. (14) and (17), the numerical recurrence formula can be used for calculating $R(t)$ at any time instant $t_j = j\cdot\Delta t$ $(j = 1, 2, ...)$. The $R(t_j)$ can be given by

$$R(t_j)\approx R(t_{j-1})+\frac{\prod_{i=1}^n(\varphi_{iU}-\varphi_{iL})\Delta t}{2^{n+1}}\underbrace{\sum_{k=1}^m A_k\cdots\left\{\sum_{k=1}^m A_k\right.}_{n}\left.\left\{M(t_{j-1},\boldsymbol{\varphi})\left[H(t_{j-1},\boldsymbol{\varphi})+H(t_j,\boldsymbol{\varphi})\right] f_\Phi(\boldsymbol{\varphi})\right\}_{\varphi_1=\varphi_{1k}}\right\}_{\ddots\,\varphi_n=\varphi_{nk}} \tag{18}$$

where $M(t_{j-1},\varphi) = M(t_{j-2},\varphi)\left(1+\frac{[H(t_{j-2},\varphi)+H(t_{j-1},\varphi)]}{2}\Delta t\right)$, $t_0 = 0$, $R(0) = 1$, and $M(t_0,\varphi) = 1$.

The proposed dynamic reliability calculation method is summarized as follows:

Step 1: Establish the corresponding dynamic reliability model under strength degradation according to the definition of dynamic reliability;
Step 2: Identify the working condition, including PDF of the continuous working stress, the regularity of strength degradation, the density of shock load and the PDF of the amplitudes;
Step 3: Select the corresponding Gauss-Legendre quadrature formula to calculate the dynamic reliability.

5. Numerical examples

In this section, the contact fatigue reliability of a three-stage spur gear reducer, shown in Fig. 3 [36], is calculated under different conditions. Case 1 is for deterministic strength degradation and a homogeneous Poisson process shock load, Case 2 is for stochastic strength degradation and a homogeneous Poisson process shock load, and Case 3 is for stochastic strength degradation and a non-homogeneous Poisson process shock load.

Partial parameters of the reducer are listed in Table 2. For gear 3, the Hertz contact stress of the tooth surface is estimated as [37]

$$\sigma_H = C_p\sqrt{\frac{F_{t3}}{b_3 d_{g3} I}K_v K_o K_m} \tag{19}$$

where σ_H is the Hertz contact stress, C_p is the elastic coefficient of the material, F_{t3} is the tangential force of gear 3, b_3 and d_{g3} are the face width and the diameter of gear 3, respectively, K_v is the velocity factor, K_o is the overload factor, K_m is the mounting factor, and I is a geometry factor given by

$$I = \frac{d_{g3}}{2(d_{g3}+d_{p3})}\sin\alpha\cos\alpha \tag{20}$$

where α is the pressure angle of pitch circle, d_{g3} and d_{p3} are the pitch diameters of gear 3 and pinion 3, respectively.

Since each gear set provides torque multiplication, the tangential forces of gear 3 can be expressed as

$$F_{t3} = \frac{2T_{in}}{d_{p3}}\times\frac{d_{g1}d_{g2}}{d_{p1}d_{p2}} \tag{21}$$

where F_{t3} is the tangential forces of gear 3, T_{in} is the driving torque, d_{g1} and d_{p1} are the pitch diameters of gear 1 and pinion 1, respectively, d_{g2} and d_{p2} are the pitch diameters of gear 2 and pinion 2, respectively.

Combining Eqs. (19)–(21) yields

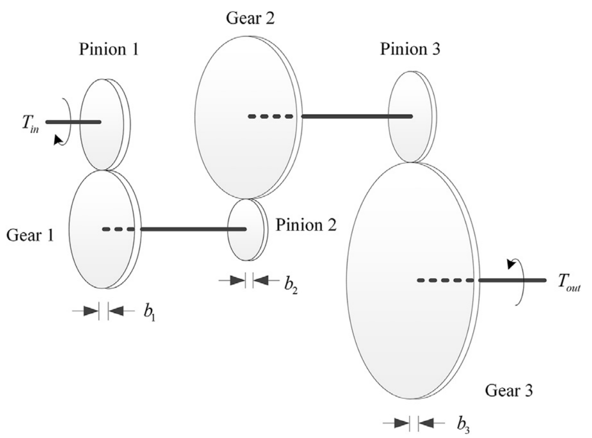

Fig. 3. A three-stage spur gear reducer.

Table 2
Partial parameters of the reducer.

Description	Symbol	Mean	Standard deviation	Distribution type	Units
Driving torque	T_{in}	108	11	Normal	N•m
Pressure angle on pitch circle	α	20	0	/	degree
Velocity factor	K_v	2.0	0	/	none
Overload factor	K_o	1.0	0	/	none
Mounting factor	K_m	1.6	0	/	none
Face width of gear 3	b_3	15	2.0	Normal	mm
Elastic coefficient	C_p	19.1	2.0	Normal	$(\mathrm{MPa})^{1/2}$
Pitch diameter of gear 1	d_{g1}	50	5.0	Normal	mm
Pitch diameter of gear 2	d_{g2}	66	6.6	Normal	mm
Pitch diameter of gear 3	d_{g3}	85	8.5	Normal	mm
Pitch diameter of pinion 1	d_{p1}	30	1.5	Normal	mm
Pitch diameter of pinion 2	d_{p2}	22	2.0	Normal	mm
Pitch diameter of pinion 3	d_{p3}	30	1.0	Normal	mm

$$\sigma_H = C_p \sqrt{\frac{4T_{in} d_{g1} d_{g2}(d_{g3} + d_{p3})}{b_3 d_{p1} d_{p2} d_{p3} d_{g3}^2 \sin\alpha\cos\alpha} K_v K_o K_m} \tag{22}$$

Monte Carlo simulation is used to get the sample points and the contact stress is normally distributed with mean 526.8 MPa and standard deviation 42.5 MPa. Then three different cases are discussed to demonstrate the applicability of the proposed method.

Case 1: Deterministic strength degradation and homogeneous Poisson process shocks

For the reasons of fatigue or aging, the strength of a gear may decrease with time. For deterministic strength degradation, assume that the strength can be modeled as $S(\Phi, t) = \varphi_0(1 - 0.00025t)$ and the initial strength φ_0 is 800 MPa, and then for a given time instant t, $S(\Phi, t) = \varphi_0(1 - 0.00025t) = 800 - 0.2t$ is a constant. The arrivals of shock loads follow a homogeneous Poisson process with intensity function $\lambda(t) = 1.0\ \mathrm{hr}^{-1}$, the amplitudes of shock loads L_s follow a normal distribution with mean value 100 MPa and standard deviation 20 MPa. Considering the uncertainty of working environment the continuous working load is modeled as $L_o(\mathbf{C}, t) = C(1 + 0.0001t)$, where C follows a normal distribution with mean value $\mu_C = 526.8$ MPa, and the standard deviation MPa. According to the additivity of normal distribution, $L_{o+s}(\mathbf{C}, t)$ follows a normal distribution. And the mean value and standard deviation can be respectively calculated as

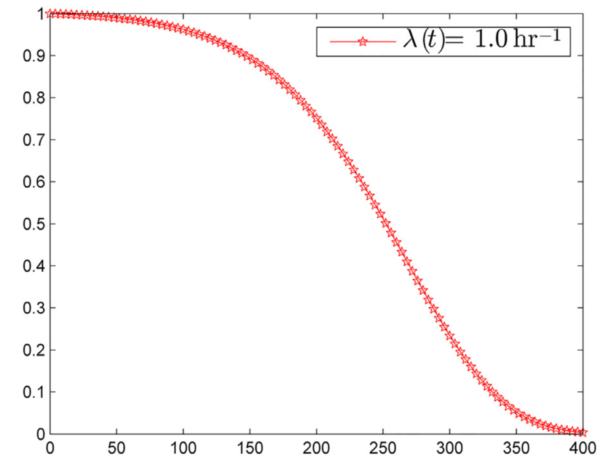

Fig. 4. Reliability curve between $R(t)$ and t.

$$\mu_{L_{o+s}}(t) = 626.8 + 0.05268t\ \mathrm{MPa}, \quad \sigma_{L_{o+s}}(t) = \sqrt{42.5^2 \cdot (1 + 0.0001t)^2 + 400}\ \mathrm{MPa}$$

If a variable x follows a normal distribution $N(\mu, \sigma^2)$, then the probability that x exceeds the interval $[\mu - 3\sigma, \mu + 3\sigma]$ and $[\mu - 6\sigma, \mu + 6\sigma]$ are no more than 0.3% and 2e-9, respectively [38]. The "six sigma" (6σ) rule is used for simplicity. Combining with Eq. (7), we then have

$$\begin{cases} f_1(t) = \int_0^t 1 \times \left\{ \int_{\mu_{L_{o+s}}(\xi) - 6\sigma_{L_{o+s}}(\xi)}^{800-0.2\xi} \frac{1}{\sqrt{2\pi}\sigma_{L_{o+s}}(\xi)} e^{-\frac{[C-\mu_{L_{o+s}}(\xi)]^2}{2\times[\sigma_{L_{o+s}}(\xi)]^2}} \mathrm{d}C - 1 \right\} \mathrm{d}\xi \\ R(t) = e^{f_1(t)} \end{cases} \tag{23}$$

Direct integral is used to Eq. (23) and the reliability curve is shown in Fig. 4.

Generally, different initial strengths will have different reliability curves. For the sake of comparisons, the reliability curves corresponding to initial strengths 720 MPa, 800 MPa, and 850 MPa are drawn in Fig. 5.

For different $\lambda(t)$, the relationship between $R(t)$ and t are shown in Fig. 6.

Figs. 5 and 6 show that the shape and the scale of reliability curve change with the initial strength φ_0 and the intensity $\lambda(t)$. Therefore, for the reliability curve under deterministic strength degradation and

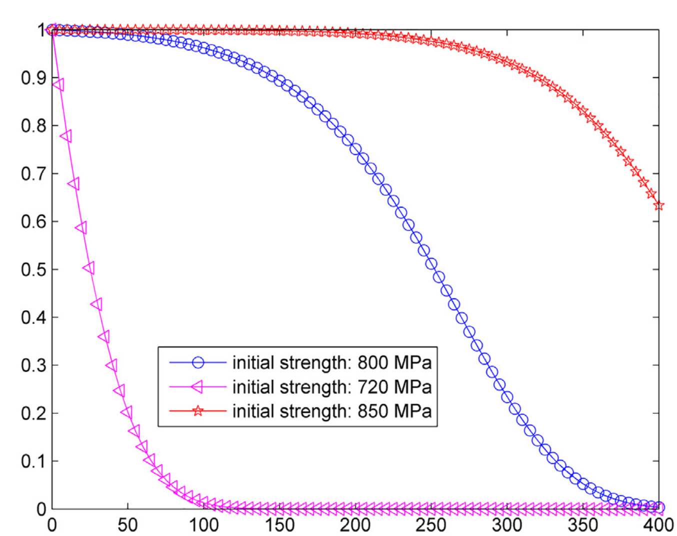

Fig. 5. Reliability curves corresponding to different initial strengths.

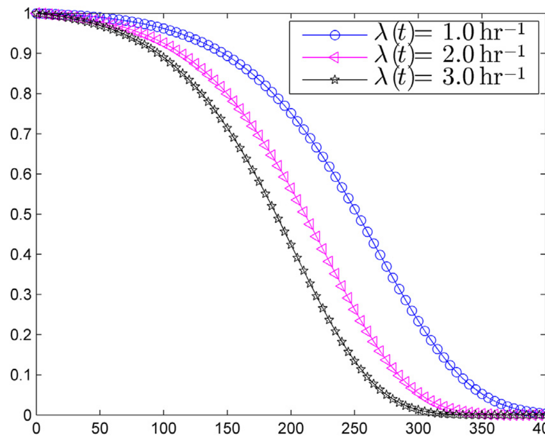

Fig. 6. Reliability curve for different $\lambda(t)$.

homogeneous Poisson process shocks, φ_0 and $\lambda(t)$ can be regarded as the shape parameter and the scale parameter, respectively.

Case 2: Stochastic strength degradation and homogeneous Poisson process shocks

For stochastic strength degradation, assume that the strength can be expressed as $S(\Phi, t) = \varphi_0(1 - 0.00025t)$, where φ_0 follows a normal distribution with the mean value $\mu_{\varphi_0} = 800$ MPa and the standard deviation $\sigma_{\varphi_0} = 20$ MPa. For a given time instant t, $S(\Phi, t) = \varphi_0(1 - 0.00025t)$ is a random variable. The other data are the same as Case 1.

According to the "six sigma" rule, the lower and upper bounds for integration variable φ are $\mu_{\varphi_0} - 6\sigma_{\varphi_0} = 680$ MPa and $\mu_{\varphi_0} + 6\sigma_{\varphi_0} = 920$ MPa, respectively. Eq. (8) is changed into

$$\begin{cases} f_2(\varphi, t) = \int_0^t 1 \times \left\{ \int_{\mu_{Lo+s}(\xi)-6\sigma_{Lo+s}(\xi)}^{\varphi(1-0.00025\xi)} \frac{1}{\sqrt{2\pi}\sigma_{Lo+s}(\xi)} e^{-\frac{[C-\mu_{Lo+s}(\xi)]^2}{2\times[\sigma_{Lo+s}(\xi)]^2}} \mathrm{d}C - 1 \right\} \mathrm{d}\xi \\ R(t) = \int_{680}^{920} e^{f_2(\varphi,t)} \frac{1}{\sqrt{2\pi}\times 20} e^{-\frac{(\varphi-800)^2}{2\times 20^2}} \mathrm{d}\varphi \end{cases} \tag{24}$$

Using Eq. (18) and to set $\Delta t = 0.1$, we obtained the system reliability at any time instant $t = n{\cdot}\Delta t$. To verify the accuracy of the proposed method, Monte Carlo simulation is used for comparisons and the reliability curves are shown in Fig. 7.

As is shown in Fig. 7, it has shown the high accuracy of the proposed method.

Case 3: Stochastic strength degradation and nonhomogeneous Poisson process shocks

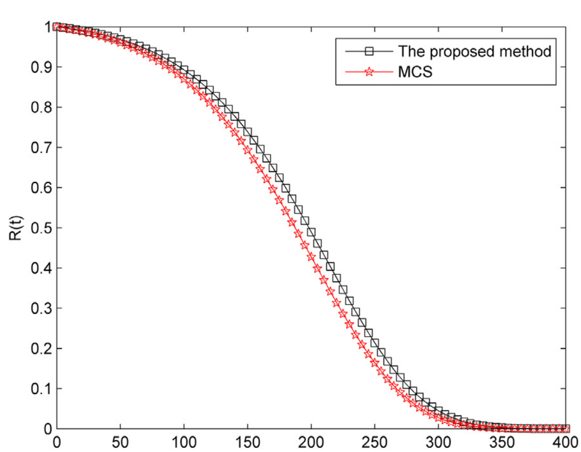

Fig. 7. Reliability curve between $R(t)$ and t for different methods.

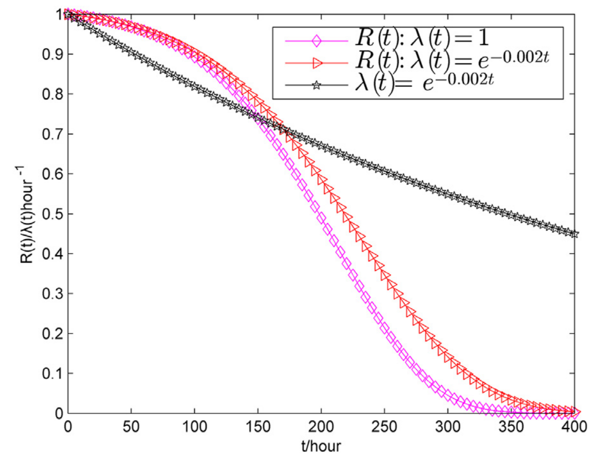

Fig. 8. $\lambda(t)$ and reliability curves under different intensity functions.

Assume that the shock load follows a nonhomogeneous Poisson process with intensity function $\lambda(t) = e^{-0.002t}$ hr^{-1}, and the other data are the same as Case 2.

Eq. (24) is rewritten as

$$\begin{cases} f_3(\varphi, t) = \int_0^t e^{-0.002\xi} \times \left\{ \int_{\mu_{Lo+s}(\xi)-6\sigma_{Lo+s}(\xi)}^{\varphi\cdot(1-0.00025\xi)} \frac{1}{\sqrt{2\pi}\sigma_{Lo+s}(\xi)} e^{-\frac{[C-\mu_{Lo+s}(\xi)]^2}{2\times[\sigma_{Lo+s}(\xi)]^2}} \mathrm{d}C \right. \\ \qquad \left. - 1 \right\} \mathrm{d}\xi \\ R(t) = \int_{680}^{920} e^{f_3(\varphi,t)} \frac{1}{\sqrt{2\pi}\times 20} e^{-\frac{(\varphi-800)^2}{2\times 20^2}} \mathrm{d}\varphi \end{cases} \tag{25}$$

Set $\Delta t = 0.1$ hr^{-1}, and Eq. (18) is used for calculating system reliability. The intensity function of nonhomogeneous Poisson process and the reliability curves under different intensity functions are drawn in Fig. 8.

Fig. 8 shows that as the intensity increases, the reliability decreases quickly and preventive maintenance is desirable to keep the high reliability of the system.

6. Conclusions

Based on the SSI theory, a generalized dynamic reliability model is proposed for considering uncertain strength deterioration and complex load condition. The main advantage of the proposed model is that it can predict the dynamic reliability of the system under complex load, deterministic strength degradation or stochastic strength degradation. For stochastic strength degradation, it is difficult to obtain the explicit system reliability model. The "Six sigma" rule and Gauss-Legendre quadrature formula are used for approximating the system reliability, which transform the integral into the sum of a series of polynomials with high accuracy. Monte Carlo simulation is used for the comparisons to demonstrate the accuracy of the proposed method. The results have demonstrated the feasibility of the proposed method. A numerical example under different profiles is given to illustrate the applicability of the proposed method. The studies show that for deterministic strength degradation, the initial strength and Poisson intensity can be regarded as the shape parameter and scale parameter. For a system of which the strength follows a stochastic degradation process and the shock follows a homogeneous or nonhomogeneous Poisson process, given the required system reliability, pro-active maintenance can be implemented before the system enters the down state according to the reliability curves to maintain a high system reliability. In this paper, the strength and the stress are supposed to be statistically independent and the amplitude of shocks is normally distributed. Future work will consider the correlations between the strength and the stress as well as stochastic process of amplitude.

Acknowledgements

The authors greatly acknowledge support from the National Natural Science Foundation of China under contract number 51775090.

References

[1] Zheng B, Huang HZ, Guo W, Li YF, Mi J. Fault diagnosis method based on supervised particle swarm optimization classification algorithm. Intell Data Anal 2018;22(1):191–210.
[2] Li YF, Mi J, Liu Y, Yang YJ, Huang HZ. Dynamic fault tree analysis based on continuous-time Bayesian networks under fuzzy numbers. Proc Inst Mech Eng Part O J Risk Reliab 2015;229(6):530–41.
[3] Li XY, Huang HZ, Li YF. Reliability Analysis of phased mission system with non-exponential and partially repairable components. Reliab Eng Syst Safe 2018;175:119–27.
[4] Cox DR. The theory of stochastic processes. London: Routledge; 2017.
[5] Skiadas CH, Skiadas C. Exploring the state of a stochastic system via stochastic simulations: An interesting inversion problem and the health state function. Methodol Comput Appl 2015;17(4):973–82.
[6] Jiang C, Huang XP, Han X, Zhang D. A time-variant reliability analysis method based on stochastic process discretization. J Mech Des 2014;136(9):091009.
[7] Coleman JJ. Reliability of aircraft structures in resisting chance failure. Oper Res 1959;7(5):639–45.
[8] Crandall SH, Chandiramani KL, Cook RG. Some first-passage problems in random vibration. J Appl Mech T ASME 1966;33(3):532–8.
[9] Spanos PD, Kougioumtzoglou IA. Galerkin scheme based determination of first-passage probability of nonlinear system response. Struct Infrastruct Eng 2014;10(10):1285–94.
[10] Rackwitz R. Computational techniques in stationary and non-stationary load combination—a review and some extensions. J Struct Eng ASCE 1998;25(1):1–20.
[11] Melchers RE, Beck AT. Structural reliability analysis and prediction. John Wiley & Sons; 2018.
[12] Hu Z, Du X. Time-dependent reliability analysis with joint upcrossing rates. Struct Multidiscip O 2013;48(5):893–907.
[13] Jiang C, Wei XP, Huang ZL, et al. An outcrossing rate model and its efficient calculation for time-dependent system reliability analysis. J Mech Design 2017;139(4):041402.
[14] Andrieu-Renaud C, Sudret B, Lemaire M. The PHI2 method: a way to compute time-variant reliability. Reliab Eng Syst Safe 2004;84(1):75–86.
[15] Zhang D, Han X, Jiang C, Liu J, Li Q. Time-dependent reliability analysis through response surface method. J Mech Des 2017;139(4):041404.
[16] Li J, Mourelatos ZP. Time-dependent reliability estimation for dynamic problems using a niching genetic algorithm. J Mech Des 2009;131(7):071009.
[17] Singh A, Mourelatos ZP, Nikolaidis E. An importance sampling approach for time-dependent reliability. Proceedings of the ASME 2011 International Design Engineering Technical Conferences and Computers and Information in Engineering Conference, IDETC/CIE. 2011. p. 28–31. Aug. 28-31.
[18] Jiang C, Huang XP, Han X, Zhang DQ. A time-variant reliability analysis method based on stochastic process discretization. J Mech Des 2014;136(9):091009.
[19] Wang Z, Zhang X, Huang HZ, Mourelatos ZP. A simulation method to estimate two types of time-varying failure rate of dynamic systems. J Mech Des 2016;138(12):121404.
[20] Peng W, Li YF, Yang YJ, Mi J, Huang HZ. Bayesian degradation analysis with inverse Gaussian process models under time-varying degradation rates. IEEE Trans Reliab 2017;66(1):84–96.
[21] Mourelatos ZP, Majcher M, Pandey V, Baseski I. Time-dependent reliability analysis using the total probability theorem. J Mech Des 2015;137(3):031405.
[22] Hu Z, Du X. A sampling approach to extreme value distribution for time-dependent reliability analysis. J Mech Des 2013;135(7):071003.
[23] Mi J, Li YF, Liu Y, Yang YJ, Huang HZ. Belief universal generating function analysis of multi-state systems under epistemic uncertainty and common cause failures. IEEE Trans Reliab 2015;64(4):1300–9.
[24] Wang Z, Wang P. A nested extreme response surface approach for time-dependent reliability-based design optimization. J Mech Des 2012;134(12):121007.
[25] Zayed A, Garbatov Y, Soares CG. Time variant reliability assessment of ship structures with fast integration techniques. Probabilist Eng Mech 2013;32:93–102.
[26] Mi J, Li YF, Peng W, Huang HZ. Reliability analysis of complex multi-state system with common cause failure based on evidential networks. Reliab Eng Syst Safe 2018;174:71–81.
[27] Liu Z, Yu L, Li YF, Mi J, Huang HZ. Comparisons of two non-probabilistic structural reliability analysis methods for aero-engine turbine disk. Int J Turbo Jet Engines 2017;34(3):295–303.
[28] Wang Z, Wang P. A double-loop adaptive sampling approach for sensitivity-free dynamic reliability analysis. Reliab Eng Syst Safe 2015;142:346–56.
[29] Guo J, Li YF, Zheng B, Huang HZ. Bayesian degradation assessment of CNC machine tools considering unit non-homogeneity. J Mech Sci Technol 2018;32(6):2479–85.
[30] Park JH. Time-dependent reliability of wireless networks with dependent failures. Reliab Eng Syst Safe 2017;165:47–61.
[31] Mi J, Li YF, Yang YJ, Peng W, Huang HZ. Reliability assessment of complex electromechanical systems under epistemic uncertainty. Reliab Eng Syst Safe 2016;152:1–15.
[32] Li XY, Huang HZ, Li YF, Zio E. Reliability assessment of multi-state phased mission system with non-repairable multi-state components. Appl Math Model 2018;61:181–99.
[33] Yang YJ, Peng W, Zhu SP, Huang HZ. A Bayesian approach for sealing reliability analysis considering the non-competing relationship of multiple degradation processes. Ekcsploatacja i Niezawodnosc – Maint Reliab 2016;18(1):10–5.
[34] Golub GH, Welsch JH. Calculation of Gauss quadrature rules. Math Comput 1969;23(106):221–30.
[35] Swarztrauber PN. On computing the points and weights for Gauss-Legendre quadrature. Siam J Sci Comput 2003;24(3):945–54.
[36] Thompson DF, Gupta S, Shukla A. Tradeoff analysis in minimum volume design of multi-stage spur gear reduction units. Mech Mach Theory 2000;35(5):609–27.
[37] Juvinall RC, Marshek KM. Fundamentals of machine component design. New York: John Wiley & Sons; 2006.
[38] Ross SM. Introduction to probability and statistics for engineers and scientists. US: Academic Press; 2014.